Kaon and Proton Spectra from STAR 4.5 GeV Fixed-Target Au Halo on Al Beampipe
Elena Amparo

Abstract

Fixed-target configurations extend the reach of the BES to lower energies. Spectra show the distribution of particle yields over 2-D momentum space. Raw kaon and proton spectra were produced for 4.5 GeV fixed target collisions of the Au halo on Al beampipe. Proton spectra showed a negative exponential relationship between yield and m_T-m_0, as expected. Kaon spectra showed a roughly exponential falloff but contained much larger fluctuations due to the small yield and difficulty identifying particles with overlapping dE/dx curves. Spectra are used to calculate temperature and chemical potential.

Introduction

STAR is the Solenoidal Tracker At RHIC, the Relativistic Heavy Ion Collider. Heavy ion collisions are used to produce a quark gluon plasma and study its properties. The Beam Energy Scan (BES) at STAR was designed to study the phase transition of nuclear matter from a hadronic gas, where quarks and gluons are confined inside of hadrons, to a quark-gluon plasma (QGP) where free quarks and gluons exist, with the aim of locating a first-order phase transition and the critical point where both phases exist simultaneously. The BES operates by colliding beams of heavy nuclei over a range of collision energies and characterizing the produced particles. Beam-on-beam runs provide data down to $\sqrt{s_{NN}}$ = 7.7 GeV center-of-mass energy. Data from lower-energy collisions are necessary to investigate the threshold of QGP formation; however, the beams become difficult to focus at lower energies, and beam-on-beam systems become inefficient at producing a large sample size of collisions. Thus, the BES was expanded to include fixed target collisions. Aiming a beam at a stationary fixed target produces collisions with approximately half the energy of the beam, allowing the BES to reach center-of-mass energies as low as a few GeV.

The purpose of this project is to produce kaon and proton spectra from the background collisions of the gold beam halo on the aluminum beampipe from the 19.6 GeV beam-on-beam run, which produced background fixed-target collisions with 4.5 GeV center-of-mass energy. Background collisions of the beam halo on the beampipe were the first fixed-target collisions to be analyzed as part of the BES, and were used in a proof-of-principle study to justify the installation of a gold target in the detector. The gold target allows fixed-target collisions to be produced directly, instead of as a byproduct of beam-on-beam collisions. The older data from background collisions remain relevant as a comparison point for data obtained using the gold target. The results from this retrospective analysis will complement more recent aluminum-on-gold data, because each system has better detector acceptance near the rapidity of the target, which is zero in the lab frame.

Nuclear Matter Phase Diagram
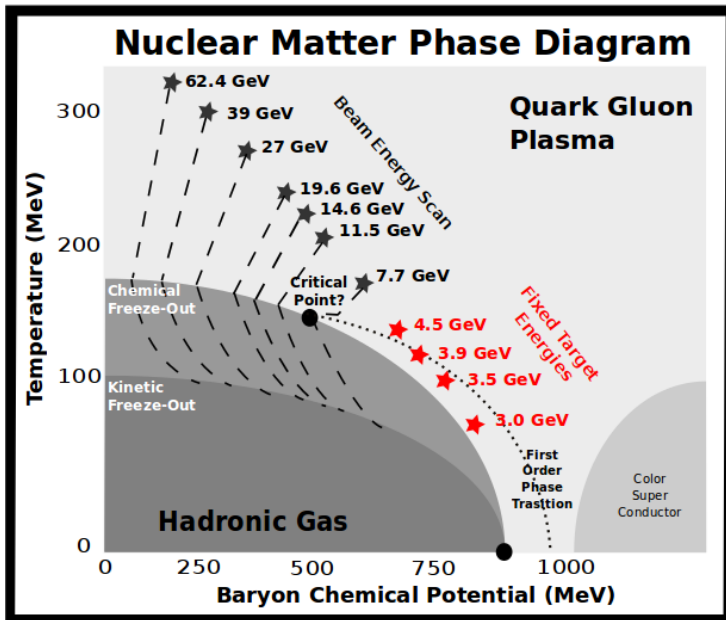
Fig. 1 (Haag, Flores et al.)

Nuclear matter is characterized in terms of temperature and baryon chemical potential. Fixed-target configurations extend the reach of the BES to lower energies, corresponding to lower temperatures and higher baryon chemical potentials.

Detector systems

The particles produced and scattered by a nuclear collision are studied using two different systems in the STAR detector.

The Time Projection Chamber (TPC) tracks the path of particles through the detector, from which the momentum can be calculated. It also measures ionization energy loss, which is used for particle identification. The TPC is a chamber filled with P-10 gas, a combination of 90% argon and 10% methane. The chamber contains uniform electric and magnetic fields. As a charged particle travels through the TPC, it ionizes the argon by knocking off electrons. The loose electrons drift in a straight line in the z direction, parallel to the beampipe, in the uniform electric field and reach the end-cap detectors, which record their x-y position and drift time. The drift time is then used to calculate the electron's original z position. The particle's path is reconstructed by fitting the xyz positions of the drift electrons to a helix. The reconstructed path can then be used to calculate the particle's momentum. The z momentum can be calculated from the distance between revolutions, and the xy, or transverse, momentum can be calculated from the radius of the revolutions.

As a charged particle ionizes the TPC gas, it loses energy in proportion to the number of ionization events per unit distance. For a given particle species, this ionization energy loss, or dE/dx, can be predicted as a function of momentum using Bichsel curves and used for particle identification.

The second detector system is the Time of Flight (TOF) detector, a thin layer outside the TPC. The TOF detector measures the time at which particles reach this outer layer, with very fine resolution. By subtracting the time of the collision, we can obtain the particle's time of flight through the detector. Then, using the length of the reconstructed track and relativistic mechanics,

we can calculate the particle's speed and $1/\beta$, where $\beta = v/c$. For a given particle species, $1/\beta$ is a known function of momentum and can be used for particle identification.
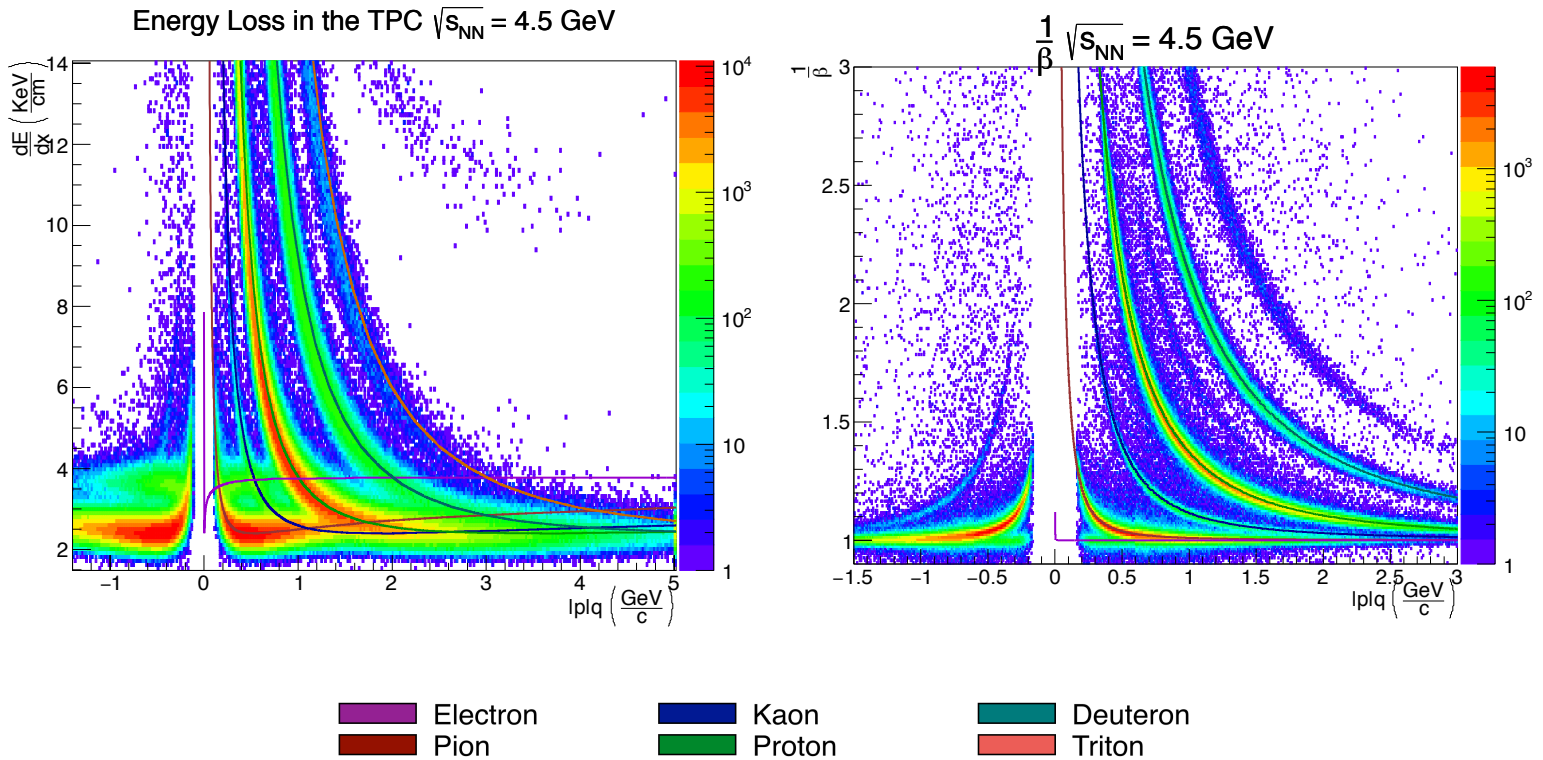
Fig. 2
Particle identification plots. The z axis corresponds to the number of tracks, or particle count. The colored lines show the theoretical dE/dx and $1/\beta$ functions for each particle. The dE/dx plot shows the overlap of the kaon curve with other particles, and the overall low yield of kaons. The $1/\beta$ plot shows that there are negative kaons but no antiprotons.

Particle Spectra

The purpose of this project is to produce kaon and proton spectra. A spectrum in general refers to an energy distribution. Particle spectra show the distribution of particle yields over momentum space. The azimuthal symmetry of the system suggests that we collapse the 3-dimensional momentum space into the 2-dimensional space of p_Z and p_T, the transverse momentum. The quantity p_Z is expressed in terms of rapidity, while transverse momentum is expressed in terms of m_T-m_0, or transverse mass minus rest mass. These variables are more useful than momentum and are a function of momentum for a given particle species.

Rapidity, abbreviated y, is a generalization of velocity, and is a more useful quantity in relativistic contexts because it is additive under the Lorentz transformation. Rapidity is given by $y = \tanh^{-1}\beta$, mapping the -1 to 1 interval of values of β to the full real line.

$$E = \sqrt{p_T^2 + p_z^2 + m_0^2} \qquad\qquad y = \tanh^{-1}(\beta) = \frac{1}{2}\ln\left(\frac{1+\beta}{1-\beta}\right) = \frac{1}{2}\ln\left(\frac{E+p_z}{E-p_z}\right)$$

The quantity m_T is the transverse mass, or the quantity of mass energy moving in the transverse direction. m_T is the independent variable in plots of particle yields. We subtract m_0, the rest mass, so that particles of different species and masses can be compared.

$$m_T - m_0 = \sqrt{p_T^2 + m_0^2} - m_0$$

Raw Data

The detector collects data at three levels: event level, vertex level, and track level. A collision triggers the detector to take data for 40 ns. An event corresponds to a trigger and contains all of the data taken during that time. Vertices correspond to individual collisions. A good event includes at least one vertex, corresponding to the initial collision of the heavy ions that triggered the detector, but it can contain multiple additional vertices corresponding to collisions that occurred before or after the detector began taking data. Tracks correspond to individual particles produced or scattered in the collisions.

Our raw data is a collection of tracks containing the reconstructed paths of particles and values for momentum, dE/dx, and 1/β. Each track belongs to a vertex, which contains the xyz coordinates of the collision. Each vertex belongs to an event. We make cuts at the event, vertex, and track level to choose only those tracks which correspond to fixed-target collisions and contain good quality data, and use these tracks in our analysis.

Data Cuts

At the event level, we chose events with at least one primary vertex. At the vertex level, we calculated the centrality of each collision, or the degree of cross-sectional overlap between the colliding nuclei, and chose the 10% most central collisions. Centrality was measured in terms of the number of produced pions. The number of pions was estimated by counting the number of tracks with dE/dx values within two standard deviations of the expected value for pions.

In order to select the beam-on-beampipe fixed-target collisions, we chose vertices with radial positions on the beampipe wall, between 2 and 5 cm. We also chose vertices with z positions between -200 and -150 cm, at the far left of the detector, and tracks with positive y, corresponding to particles traveling right. This selected particles that traveled most of the length of the detector, leaving long tracks with many data points for reliable interpolation. The choice of positive y was arbitrary; a similar cut could have been made to choose vertices at the far right of the detector with tracks traveling to the left.

At the track level, we chose tracks with at least 15 hit points in the TPC and at least 52% of hits used in the track reconstruction, in order to ensure track quality.

Data Analysis

The goal of the analysis was to produce spectra showing the distribution of kaon and proton yields over y and m_T-m_0. Particles were identified using the z variable. The z of a variable is the natural log of the ratio of the measured value of the variable to the expected value. For a given particle of interest, zTPC of a track is the log of the ratio of the track's dE/dx to the expected value of dE/dx for the particle of interest, given the track's total momentum. zTOF of a track is the log of the ratio of the track's $1/\beta$ to the expected value of $1/\beta$ for the particle of interest given the track's momentum. For the particle of interest, the expectation value of the z variable is by definition zero. We expect the z variable to be normally distributed, and the tracks corresponding to the particle of interest to follow a normal distribution centered about z=0. The tracks corresponding to other particle species follow normal distributions centered about their respective expectation values for the z variable.

$$Z_x = \ln \left(\frac{\text{measured value of } x}{\text{expected value of } x \text{ for particle of interest}} \right)$$

Rapidity and m_T-m_0 were calculated for each track assuming the mass of the particle of interest. A histogram of the z variable was produced for each combination of y and m_T-m_0 bins. Each histogram contained a set of Gaussians, each corresponding to the tracks of a particular particle species and centered about the expected value of the z variable for that particle species. Separate analyses were carried out for zTPC and zTOF.

The bulk of the analysis was devoted to fitting Gaussians to the particle yields. When the z variable for the particle of interest was well-separated from other particles, a single Gaussian fit could be applied over the appropriate interval. Fitting became challenging in momenta where different particles overlapped. This was primarily an issue with zTPC. Figure 2 shows that $1/\beta$ clearly distinguishes between different particle species over the full range of momenta. However, in dE/dx, kaons overlap with either electrons, pion, protons, or deuterons over a substantial range of momenta. At high momenta, all of the particles become difficult to distinguish by dE/dx.

$$f(x) = ae^{-\frac{1}{2}\left(\frac{x-b}{c}\right)^2}$$

A Gaussian function has three parameters: the amplitude, the mean, and the width. The amplitude (a) is the height of the maximum, and the mean (b) is the position of the maximum. The width (c) controls the spread of the peak, and is the standard deviation.

If the particle of interest overlapped with other particles, we included an additional Gaussian in the fit function for each additional peak. When fitting multiple Gaussians, it is most challenging to fit the width accurately. This can lead to under- or over-estimation of particle yields. One strategy for fitting widths more accurately is to fit the widths as a function of y and m_T-m_0. Widths are first estimated in a preliminary fitting round where amplitude, mean, and width are allowed to float. For each y bin, the width estimates are fit to a function of m_T-m_0. In the final fitting round, the width is fixed to the value of the fit function, while mean and amplitude are allowed to float.

Fig. 2 gives an overview of the relative yields of the different particle species as a function of total momentum. If the expectation values for two different particle species were both centered near the same Gaussian but Fig. 2 showed that one yield was lower than the other by an order of magnitude, we disregarded the lower-yield particle and fit a single Gaussian corresponding to the higher-yield particle. The total momentum for each particle species in a given y, m_T-m_0 bin can be calculated as a function of y, m_T-m_0, and m_0 for that species. Based on the evidence in Fig. 2, we disregarded antiprotons and high-momentum kaons and positrons where they overlapped with other particles with higher yields.

The protons were sufficiently well separated and had large enough yields that a single Gaussian fit could be applied. Kaon fits frequently required multiple Gaussians. A width-fitting step was incorporated into the kaon fitting algorithm but ultimately removed because there were insufficient data to fit the widths accurately.

Before attempting to fit the yield, we skipped plots where the particle of interest overlapped too much with other particles or the amplitude of the yield was too small to fit accurately. Many of the kaon plots had these characteristics and were unable to be fit.

After fitting, we calculated the raw yields by integrating the Gaussians and dividing by the bin size, the number of events, and a normalization constant. The raw yields were then plotted as a function of y and m_T-m_0 to produce the raw spectra.
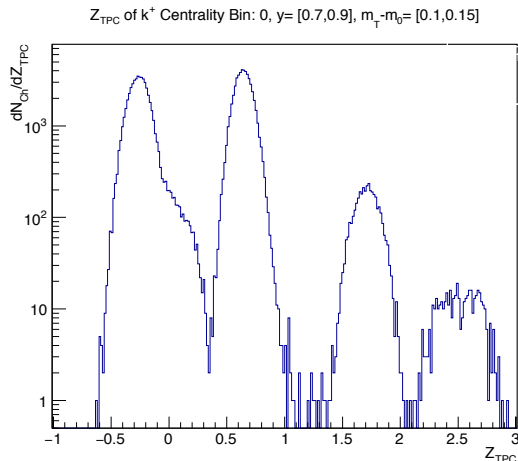
Fig 3a.
A k^+ zTPC histogram where the kaon peak, centered at z=0, cannot be fit because the kaon peak is covered by the pion peak to its left.

Z_{TPC} of k^+ Centrality Bin: 0, y= [0.5,0.7], m_T-m_0= [0,0.05]

zTPC_KaonPlus_Cent0_14_1	
Entries	114248
Mean	−0.3668
RMS	0.7439
χ^2 / ndf	342.4 / 155
p0	45 ± 1.6
p1	0.0025 ± 0.0275
p2	0.07011 ± 0.00282
p3	3487 ± 15.0
p4	−0.7773 ± 0.0006
p5	0.1453 ± 0.0004
p6	193.3 ± 4.9
p7	−0.3061 ± 0.0033
p8	0.09513 ± 0.00263
p9	1875 ± 15.0
p10	0.941 ± 0.001
p11	0.08001 ± 0.00039
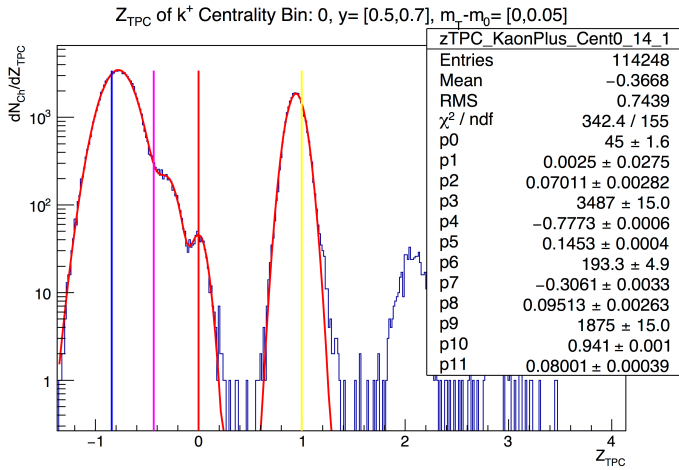
Fig 3b.
A k^+ zTPC histogram requiring fitting multiple gaussians. The colored lines show expected z values for pions, positrons, kaons, and protons respectively. The amplitude, mean, and width parameters for each Gaussian are listed consecutively.

Z_{TOF} of k^+ Centrality Bin: 0, y= [-0.1,0.1], m_T-m_0= [0.1,0.15]

zTOF_KaonPlus_Cent0_11_3	
Entries	9315
Mean	0.01122
RMS	0.4633
χ^2 / ndf	263.2 / 64
p0	18 ± 8.1
p1	0.00297 ± 0.00125
p2	0.008511 ± 0.001019
p3	394.7 ± 6.9
p4	−0.4534 ± 0.0008
p5	0.03747 ± 0.00047
p6	604.8 ± 11.5
p7	0.471 ± 0.000
p8	0.02339 ± 0.00028
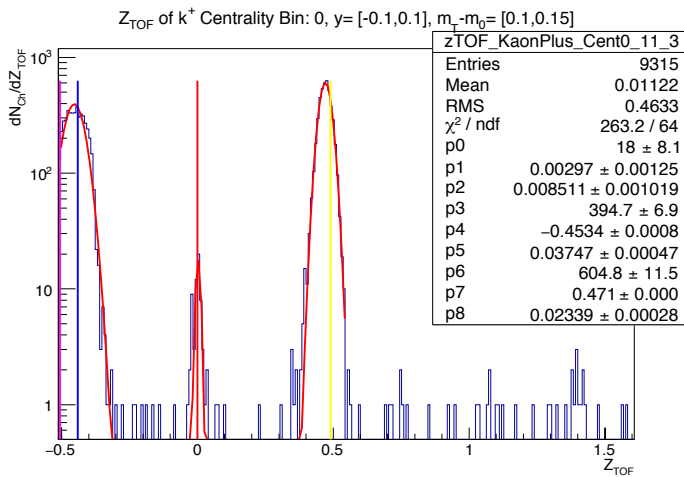
Fig 3c.
A k^+ zTOF histogram. From left to right, the pions, kaons, and protons are clearly separated.

Z_{TPC} of p Centrality Bin: 0, y= [0.5,0.7], m_T-m_0= [0.25,0.3]

zTPC_ProtonPlus_Cent0_14_6	
Entries	34574
Mean	0.05211
RMS	0.2317
χ^2 / ndf	288.1 / 35
p0	2134 ± 17.5
p1	−0.01468 ± 0.00046
p2	0.07267 ± 0.00040
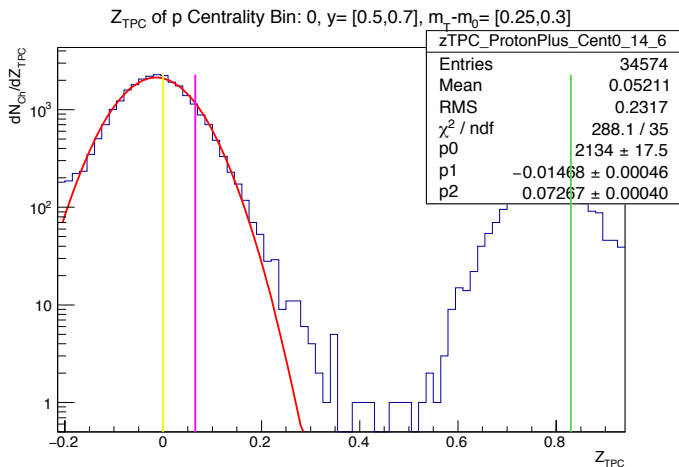
Fig 3d.
In zTPC, the proton peak is large and well-separated and can be fit using a single Gaussian. The yellow, pink, and green lines give the proton, positron, and deuteron predictions, respectively. The positrons can be disregarded based on the evidence in Fig 2.

Fig. 4a-f

● TPC +
□ TOF +

a) Proton Raw Spectra y= [-0.1,0.1]
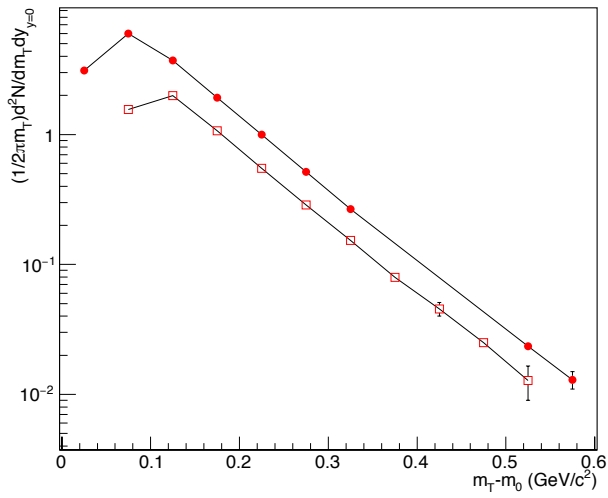
b) Proton Raw Spectra y= [0.1,0.3]
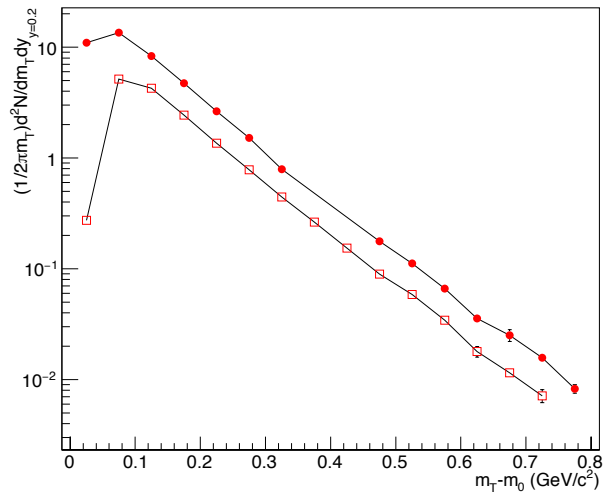
c) Proton Raw Spectra y= [0.3,0.5]
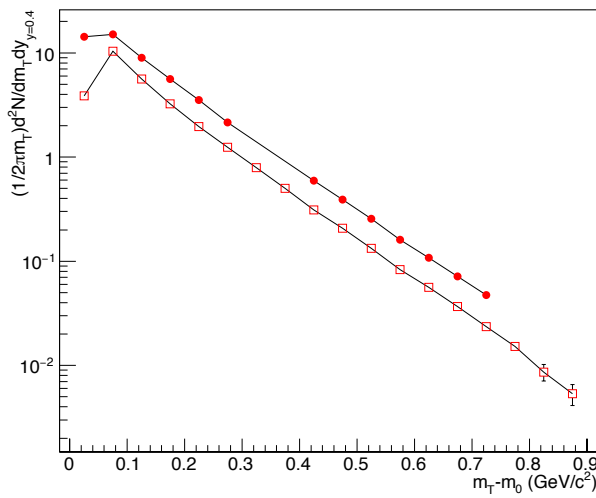
d) Proton Raw Spectra y= [0.5,0.7]
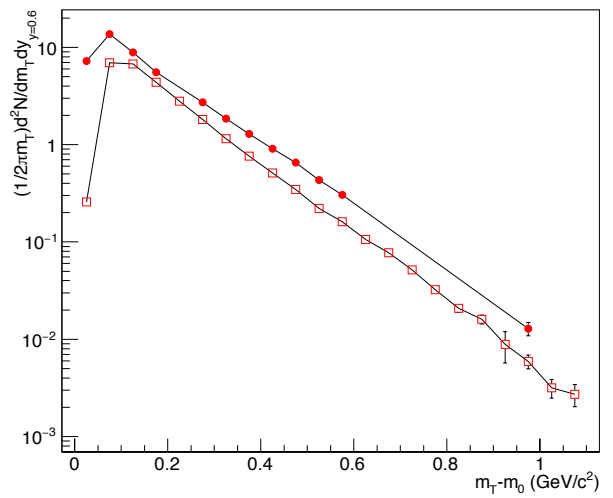
e) Proton Raw Spectra y= [0.9,1.1]
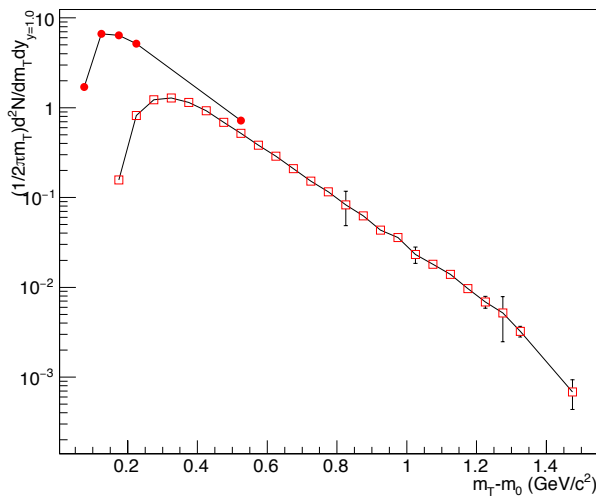
f) Proton Raw Spectra y= [1.1,1.3]
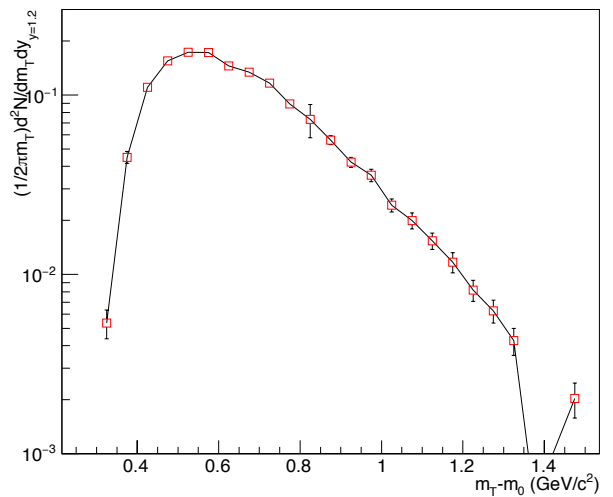
Fig. 5a-f

a) Kaon Raw Spectra y= [0.1,0.3]
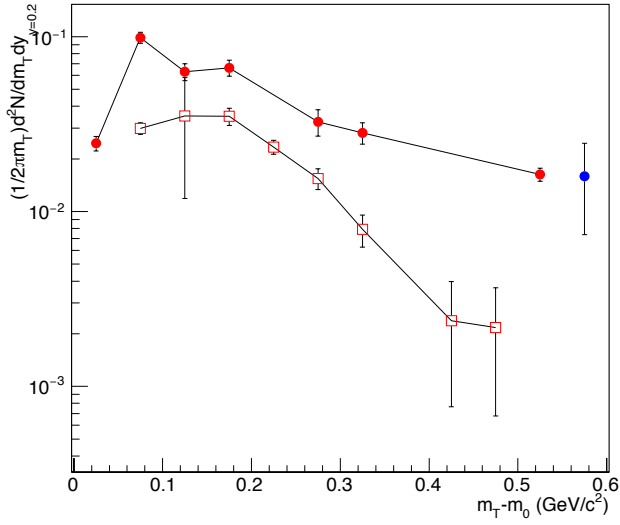
b) Kaon Raw Spectra y= [0.3,0.5]
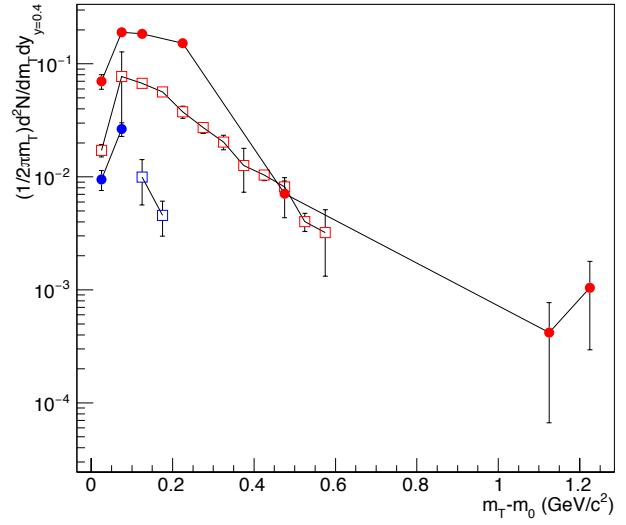
c) Kaon Raw Spectra y= [0.5,0.7]
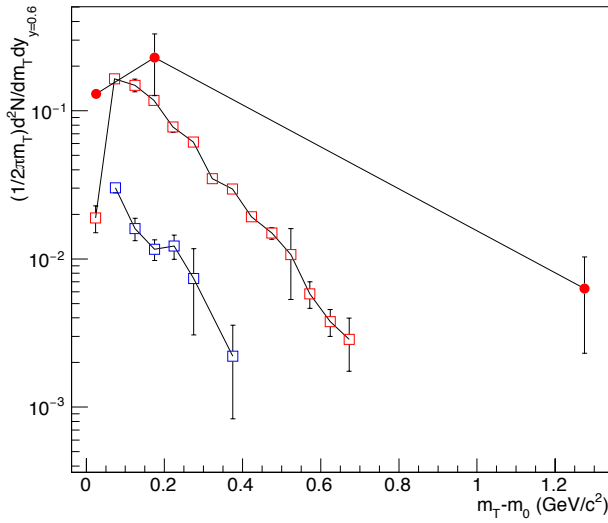
d) Kaon Raw Spectra y= [0.7,0.9]
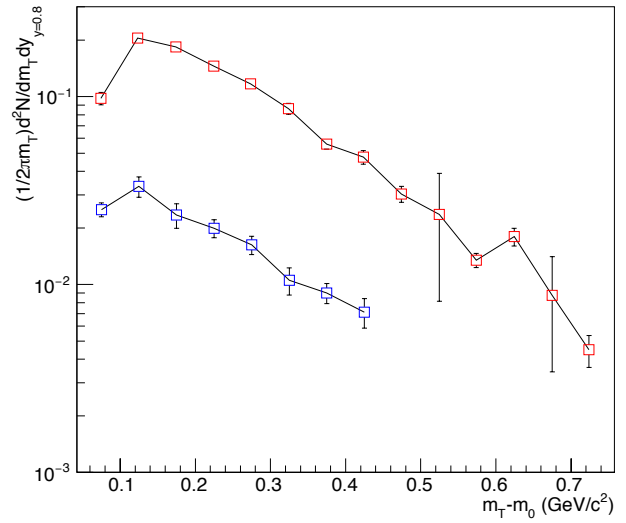
e) Kaon Raw Spectra y= [0.9,1.1]
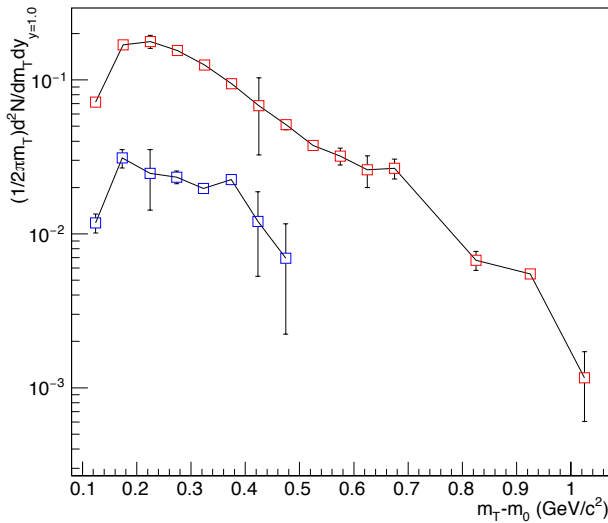
f) Kaon Raw Spectra y= [1.1,1.3]
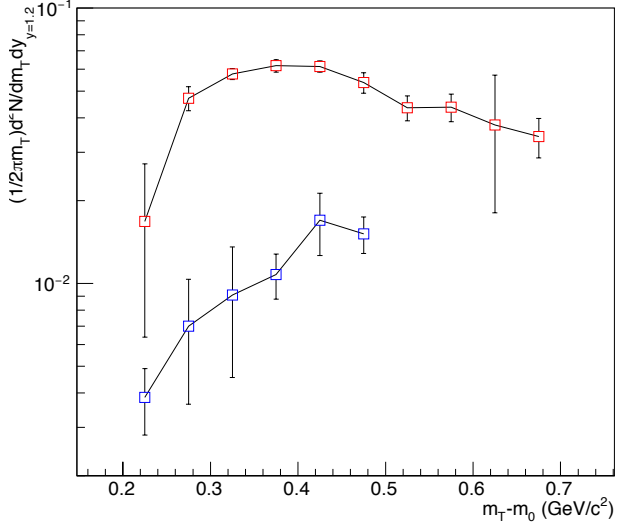
Results and Discussion

The proton spectra (Fig. 4) show a negative exponential relationship between yield and m_T-m_0, as expected. The straight lines on the log plots show constant rates of exponential decay. The kaon spectra also show an approximately exponential relationship, but they contain larger errors and show less constant rates of exponential decay. Kaons are also expected to show a constant rate of exponential decay with increasing m_T-m_0, so these spectra are not accurate.

Kaons require a strange quark, which is a heavier flavor and requires a relatively large amount of energy. As a result, strange quarks and the kaons that contain them are produced in relatively low abundance. In addition, the dE/dx curve for kaons overlaps with the curves for electrons, which have a comparable yield, and pions, which have a larger yield. Most of the kaon yields from zTPC could not be calculated because overlapping particles obscured the amplitude of the kaon peak. In addition, the yield of kaons was often too small to produce a smooth normal distribution. As a result, there were large fluctuations in the kaon spectra. The protons have a high yield and a dE/dx curve that is well separated from the other particles, making it easier to produce spectra.

Because of the difficulties distinguishing kaons using dE/dx, the kaon spectra rely primarily on TOF data. Anti-kaons, represented by blue plot points in Fig. 5, were identified almost exclusively using zTOF. In Fig. 5, the open points corresponding to zTOF data still contain large errors, but show a more constant rate of exponential decay than the zTPC points. zTOF provides more precise particle identification, and becomes particularly important at high momenta, where zTPC can no longer reliably distinguish between particles. The disappearance of the closed plot points from Fig. 4e to 4f and and 5c to 5d reflects the inability to precisely identify particles using dE/dx at high momenta. However, TOF data alone is insufficient because not all particles have enough energy to reach the outside of the TPC. Thus, the TOF tracks represent a fraction of the total yield.

Conclusion and Further Work

The kaon spectra could be improved by using a larger statistical sample. The sample size could be approximately doubled by including both tracks traveling right emerging from vertices at the left end of the detector, and tracks traveling left emerging from vertices at the right end of the detector.

The raw spectra require further corrections in order to produce corrected spectra. One of these is a detector efficiency correction. In the range of low transverse mass, many of the particles have insufficient energy to reach the tracking portion of the detector. Thus, the yield of particles with low transverse mass is undercounted. This undercounting can be seen in the low m_T-m_0 portions of Figs. 4 and 5, where the yields are lower than would be expected by extrapolating backwards from the yields at high m_T-m_0. This is corrected for using embedded tracks from Monte Carlo simulations. A TOF efficiency correction is also necessary. Not all particles have enough

momentum to reach the TOF detector, so yields calculated using zTOF represent a fraction of the total. This is seen in Figs. 4 and 5, where the zTOF yields are lower than the zTPC yields by a factor that is approximately constant in each rapidity bin. The yields calculated from zTOF are multiplied by an efficiency factor in order to correct for this. Once the efficiency correction has been applied, the yields calculated from zTOF should equal those calculated from zTPC for each rapidity and m_T-m_0 bin.

Particle spectra are used to calculate temperature and baryon chemical potential, which are then used to position data on a nuclear phase diagram. Temperature can be estimated from the m_T-m_0-dependence of the yield, and baryon chemical potential can be calculated from the temperature and the ratio of antiprotons to protons.

References

B.A. Haag, C. E. Flores, et. al. "STAR Analysis Note PSN0642: Coulomb effect in Au_Like+Al collisions at sqrt(s_NN) = 3.0, 3.5, and 4.5 GeV". URL:https://drupal.star.bnl.gov/STAR/system/files/FXT_Vc_Analysis_Note.pdf

J. Bartke, *Introduction to Relativistic Heavy Ion Physics* (World Scientific, Singapore, 2009).

K.C. Meehan, Nuclear Physics A **956**, 878 (2016).

Acknowledgements